

Design of pantograph-catenary systems by simulation

A. Bobillot^{*}, J.-P. Massat⁺, J.-P. Mentel^{*}

^{*}: Engineering Department, French Railways (SNCF), Paris, France

⁺: Research Department, French Railways (SNCF), Paris, France

Corresponding author: Adrien Bobillot (adrien.bobillot@sncf.fr), Direction de l'Ingénierie, 6 Av. François Mitterrand, 93574 La Plaine St Denis, FRANCE

Abstract

The proposed article deals with the pantograph-catenary interface, which represents one of the most critical interfaces of the railway system, especially when running with multiple pantographs. Indeed, the pantograph-catenary system is generally the first blocking point when increasing the train speed, due to the phenomenon known as the “catenary barrier” – in reference to the sound barrier – which refers to the fact that when the train speed reaches the propagation speed of the flexural waves in the contact wire a singularity emerges, creating particularly high level of fluctuations in the contact wire. When operating in a multiple unit configuration, the pantograph-catenary system is even more critical, since the trailing pantograph(s) experiences a catenary that is already swaying due to the passage of the leading pantograph.

The article presents the mechanical specificities of the pantograph-catenary system and the way the OSCAR[®] software deals with them. The resonances of the system are then analysed, and a parametric study is performed on both the pantograph and the catenary.

1. Introduction

The main aim of a catenary system is to ensure an optimum current collection for train traction. The commercial speed of trains is nowadays not limited by the engine power but one of the main challenges is to ensure a permanent contact between pantograph(s) and overhead line. Besides, statistics consolidated over Europe show an average number of more than one million minutes of delay each year in Europe related to the pantograph-catenary interface. Hence, this system deserves a deep study in order to improve future components design as well as maintenance evolution strategy.

Since 1984, SNCF has been developing Finite Element software to simulate the pantograph-catenary dynamics. The last software, named OSCAR[®] (Outil de Simulation du CAptage pour la Reconnaissance des défauts, cf. [1], [2], [3] and [6]), is a fully three-dimensional software that allows representing any kind of catenary systems (simple or compound catenary, with or without stitch wire, tramway contact lines, etc.). It takes into account all non-linearities present in the system: bumpstops, friction elements in the pantograph; non linear droppers in the catenary; contact losses at the interface. It also manages the wave propagation and the coupling of flexible structures through a load moving on a finite element mesh.

In section 2, the mechanical specificities of the pantograph-catenary system are presented, and the way the software deals with them is detailed.

Simulation is then used in section 3 to investigate the resonances that are encountered at various speeds when two pantographs are in contact with a catenary.

In section 4, a sensitivity analysis of a non linear pantograph is presented.

Finally, section 5 presents an example of catenary system optimisation and an innovation based on damping elements which improve performance in multiple unit.

2. Pantograph-catenary specificities

In the present section, we will first explain the complexity of the overhead line physics (also see [4], [5] and [9] for further information), and then, how they are handled in the OSCAR simulation software.

Firstly, the dynamic behaviour of the two flexible structures (the pantograph and the catenary) in sliding contact is very different in spite of having comparable stiffness. On one hand, the overhead line is a very long structure of wires, strongly prestressed in which bending waves propagate and, on the other hand, the pantograph is an articulated frame excited on two sides, by the train and by the overhead line, subjected to a disturbed aerodynamic environment.

The sliding contact between these two flexible structures is the main difficulty in the modelling of the pantograph catenary dynamics. In OSCAR, the overhead line is modelled using the Finite Element method and the contact with the lump mass model of pantograph is managed using the penalty method. The contact wire geometrical discretization can generate discontinuities and numerical problems in the contact force calculation when the pantograph runs from one element to another.

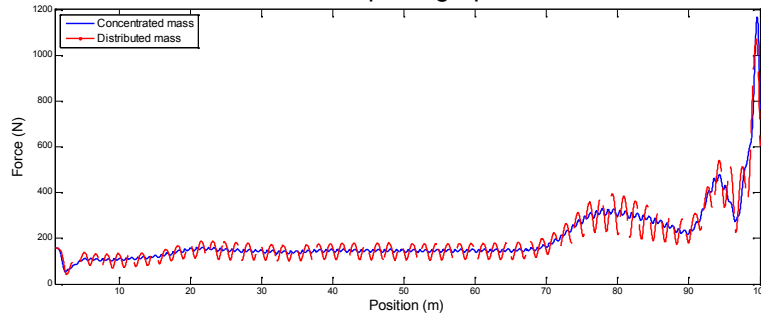


Figure 1: Effect of mass distribution on contact force fluctuation.

Figure 1 shows the artificial discontinuities that are created due to an unsuitable meshing strategy. The contact force between a lump mass model of pantograph and a stretched wire using either a concentrated mass model or a distributed mass model are shown. An amplification of the discontinuities effects can be clearly noticed when the mass is not distributed along each element.

Secondly, pantograph-overhead line dynamics is particularly sensitive to the catenary static state. Indeed, under the effect of gravity, the contact wire of the overhead line bends. Despite a huge mechanical tension (from 1 to 3 Tonnes) the contact wire deflection can reach up to 2 meters between two masts. In order to obtain an almost horizontal contact plane which allows stabilising the dynamic interaction between pantograph and overhead line, a messenger wire and droppers are added to the structure.

The computed static state is used to initialise the dynamic calculation and has consequently a very large impact on results. A realistic static state is however very complex to compute since it is highly non-linear.

Indeed, the mechanical tension on the overhead line components involves high levels of strains and geometrical deflexions. In OSCAR, the final geometry is obtained through a strongly non linear procedure which consists in solving iteratively

$$K(q_i) \cdot q_i = F_i,$$

where i is the iteration number, q is the displacement vector, K the stiffness matrix and F the force vector.

This procedure uses a progressive loading considering both the mechanical tension and the gravity. At each iteration i , the stiffness matrix is updated to consider the strains evolution in the whole overhead line and the convergence of displacements is finally ensured.

Prestressed beam formulations are used in order to take into account the additional stiffness due to mechanical tension. The equation below shows that the tension T has a big impact on the stiffness elementary matrix:

$$[K] = \sum_j \omega_j \left(\frac{1}{L} ES \frac{\partial N_u^T}{\partial r} \frac{\partial N_u}{\partial r} + \frac{1}{L} T \frac{\partial N_w^T}{\partial r} \frac{\partial N_w}{\partial r} + \frac{1}{L^3} EI \frac{\partial^2 N_w^T}{\partial r^2} \frac{\partial^2 N_w}{\partial r^2} \right)$$

The picture 3 below shows the contact wire chain shape obtained in OSCAR for a span, which is the main result of this non linear solver.

Challenge E: Bringing the territories closer together at higher speeds

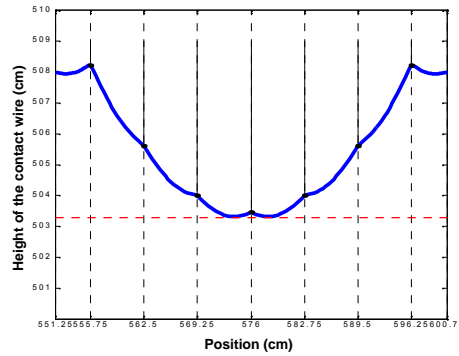


Figure 3: Static deflection of the contact wire in OSCAR

Other non-linearities appear in the system dynamics. First of all, the pantograph-catenary contact is unilateral, which can generate electrical arcs. The second non-linearity of the catenary is due to the droppers' unilaterality, as illustrated in the figure below, where one can notice that droppers do slacken at the pantograph passage.



Figure 2: Illustration of droppers' slackening.

This droppers' unilaterality must be taken into account by the simulation software, since the behaviour of the contact force strongly depends on it, as illustrated in Figure 3.

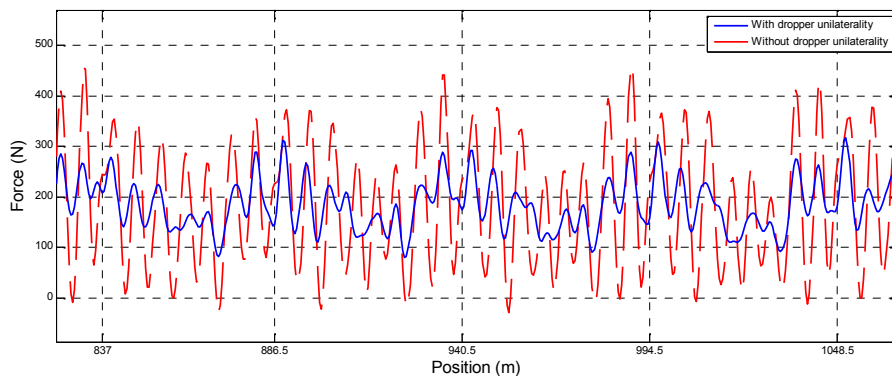


Figure 3: Comparison of contact force with and without dropper unilaterality.

Lastly, the overhead line is a wire structure of very big dimensions, strongly prestressed and very slightly damped. Bending waves propagate in the whole structure, reflect on different elements of the overhead line, and remain some minutes after the pantograph passage.

Damping modelling quality thus plays an important role in the software accuracy. OSCAR uses a damping model based on Rayleigh hypothesis with different coefficients for each part of the overhead line (contact wire, messenger wire, droppers, steady arm, stitch wire):

$$C = \sum_i \alpha_i M_i + \beta_i K_i$$

where i is the index of the overhead line component group.

In order to build the damping matrix C_i , the mass matrix M_i and the stiffness matrix K_i of each part are constructed independently and weighted by damping coefficients α_i , β_i . This distinction allows

reducing the too big damping in high frequencies of the classical Rayleigh model, thus leading to a good accuracy of the catenary oscillations. This is particularly important in case of multiple pantograph operation, when the trailing pantograph encounters a catenary that is already swaying. However, the damping in this frequency range can still be overestimated. A new improved modal damping model, easily adjustable on experiments, is in development at the moment, as described in Ref [7].

3. Analysis of the resonances

This section intends to analyse the various resonances that can be observed at various speeds for operations with two pantographs spaced by 200m.

The performance of the pantograph-catenary interaction is mainly judged through the contact force and the uplift of the contact wire at supports.

Most standards use the following quantities to assess the interaction quality:

- $\frac{\sigma}{F_m}$, which is the standard deviation of the contact force (N) divided by the mean contact force (N),
- Maximum uplift of the steady arm (cm).

In order to observe the resonances of the pantograph-catenary system, these two quantities have been extracted from simulations at various speeds. The application case consists in one of the simplest contact line systems which consists of a single Contact Wire suspended at masts by unilateral droppers forming a “Delta Suspension”, and staggered using Steady Arms (cf. figure below).

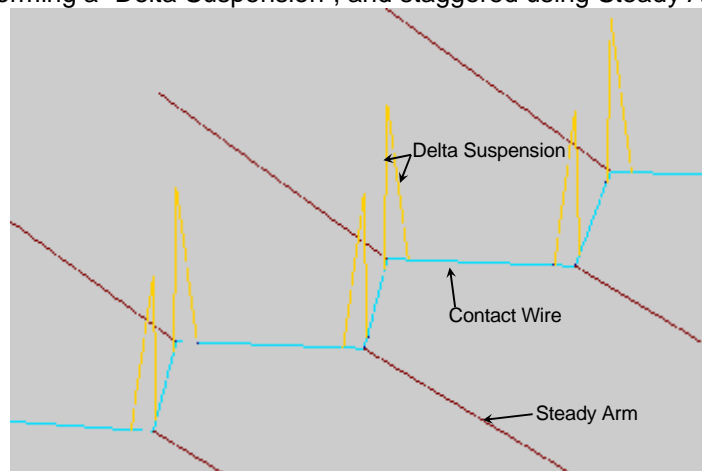


Figure 4: Schematic of the contact line system used as reference model.

The properties of this contact line are the following:

- Contact wire:
 - Section $S = 150 \text{ mm}^2$,
 - Density: $\rho = 8900 \text{ kg/m}^3$ (Copper),
 - Tension $T = 18000 \text{ N}$.
- Geometry:
 - Span lengths of 40 m and 45 m.
 - Distance between the two droppers (width of the delta): 10 m.

The approximated critical speed associated to this system is thus:

$$c = \sqrt{\frac{T}{\rho S}} = 116 \text{ m/s} = 418 \text{ km/h} .$$

This speed is also named the “catenary barrier” in reference to the sound barrier. The phenomenon of the catenary barrier is clearly visible in Figure 4, where a high resonance appears in the vicinity of $v/c=1$, corresponding to large movements of the contact wire when the pantographs are reaching the flexural waves that they generate in the contact wire.

Challenge E: Bringing the territories closer together at higher speeds

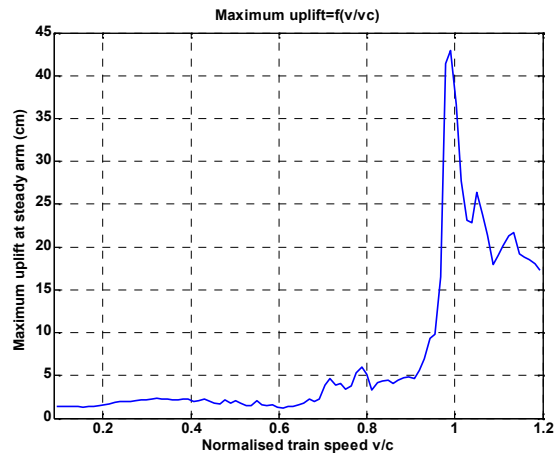


Figure 4: Maximum uplift at steady arm vs. the normalised train speed v/c .

In Figure 5, which presents σ/F_m versus the normalised train speed v/c , one can notice several resonances for the leading pantograph (as noted in [8]):

- The first resonance appears around $v/c=0.62$,
- The second resonance appears around $v/c=0.83$,
- The third peak resonance around $v/c=1$, which is linked to the catenary barrier.

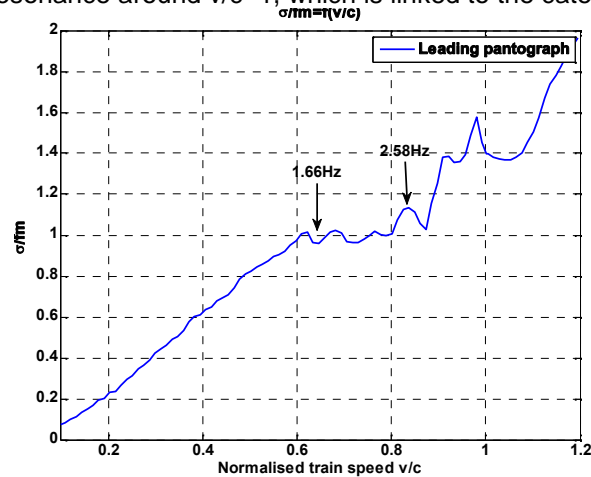


Figure 5: σ/F_m vs. the normalised train speed v/c (leading pantograph).

The first and second resonances are linked to the catenary modes. In order to check this, the first step consists in analysing the spectrum of the contact force (cf. Figure 6, top), which shows a first dynamic component at around 1.9 Hz. By transforming the frequency into an equivalent length ($L=v/f$, cf. Figure 6, bottom), one notices that this frequency corresponds to $L \approx 43\text{m}$, which is the average span length on the catenary section (span lengths range from 40 m to 45 m).

Challenge E: Bringing the territories closer together at higher speeds

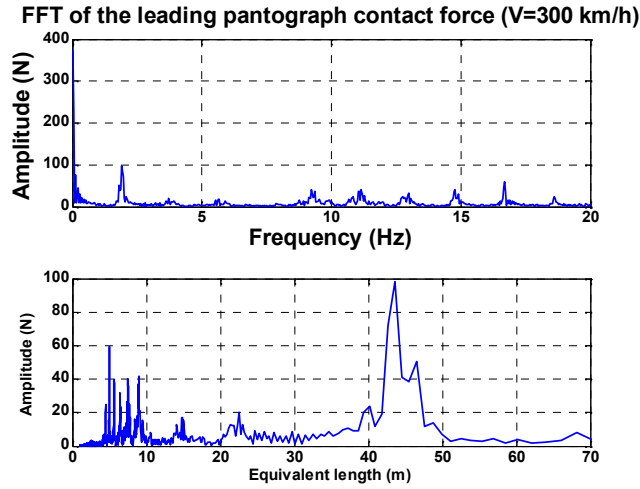


Figure 6: Top: Spectrum of the contact force at $v=300\text{km/h}$. Bottom: Spectrum of the contact force at $v=300\text{km/h}$ (equivalent lengths).

By computing the equivalent span frequency $f_{span} = v / 43$ at each train speed, it can be concluded that the first resonance is situated at around 1.66 Hz, and the second at around 2.58 Hz (cf. Figure 5). It appears that these two frequencies exactly correspond to eigen-frequencies of the catenary: 1.66 Hz indeed corresponds to the first bending mode of the contact wire between two suspensions (spaced by 35m on the 45m long span) and 2.58 Hz corresponds to the second bending mode of the contact wire between two steady arms (45m long span), as depicted in figure 7.

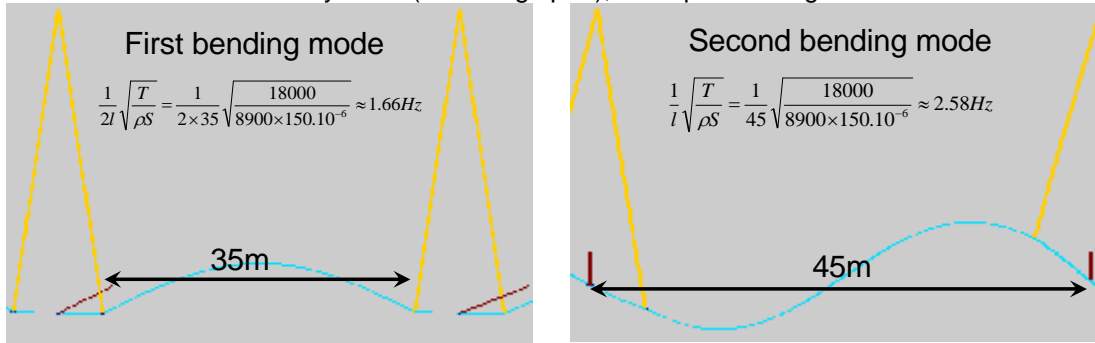


Figure 7: Some overhead contact line modes.

The resonances on the trailing pantograph (cf. Figure 8) are linked to the state of the catenary when the trailing pantograph encounters it (cf. [10] and [11]). This succession of resonances and antiresonances has been explained in [11] by the phase difference between the trailing pantograph waveform and the waveform of the contact wire oscillating at the back of the first pantograph. This analysis results in optimal and unfavourable pantograph spacings, which here correspond to optimal and unfavourable running speeds. The optimal running speed u_o , corresponding to a 180° phase difference between the waveforms, is given by:

$$\frac{u_o}{c} = \frac{D_{panto}}{L_{span}} \frac{1}{2k + 1},$$

where D_{panto} is the pantograph distance, L_{span} the average span length, c the critical speed and $k = 1, 2, 3, \dots$

Parallely, the unfavourable speed u_u , corresponding to the two waveforms in phase is given by:

$$\frac{u_u}{c} = \frac{D_{panto}}{L_{span}} \frac{1}{2k}.$$

When applying the actual values ($D_{panto} = 200\text{m}$ and $L_{span} = 43\text{m}$), one obtains the values summarised in the table below:

k	u_o/c	u_u/c
1	1.55	2.33
2	0.93	1.16

Challenge E: Bringing the territories closer together at higher speeds

3	0.66	0.78
4	0.52	0.58
5	0.42	0.47

Table 1: u_o/c and u_u/c .

These values u_u/c and u_o/c , indicated as vertical bars in figure 8 (in red and in black, respectively), correlate very well with the peaks and troughs in the σ/fm curve. This confirms the relevancy of this simple analysis, even if other phenomena are implied in the pantograph-catenary interaction quality, as show the complex shape of the σ/fm curve.

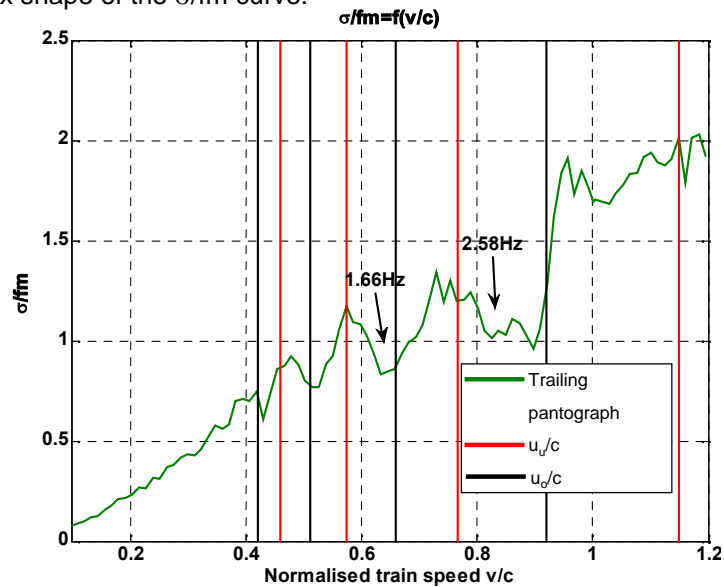


Figure 8: σ/F_m vs. the normalised train speed v/c (trailing pantograph).

4. Non linear pantograph analysis

This section presents a sensitivity analysis of a non-linear pantograph model.

The most usual pantograph models for pantograph-catenary interaction are lump mass models. These simplified models are generally built from rough design considerations and correlated with an Experimental Modal Analysis performed in laboratories. The number of degrees of freedom equals the modes taken into account and thus defines the model frequency range of validity. As the only aim is to reproduce the dynamic behaviour of the pantograph in this specific range, the geometrical information is lost.

However, construction parameters are used as much as possible in the model to allow sensitivity study or systems optimizations. As shown in Figure 7, the mass M_3 of the upper stage of 3 lump mass models is very close to the real physical mass of the bow, while C_1 and K_1 are directly linked to the characteristics of the damper situated at bottom of the actual pantograph.

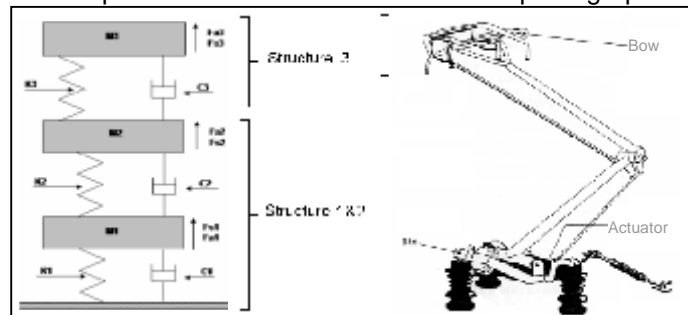


Figure 7: Physical correspondence between lump-mass model and real pantograph.

Within OSCAR, several types of lump mass models can be used (cf. Figure 10) depending on the application.

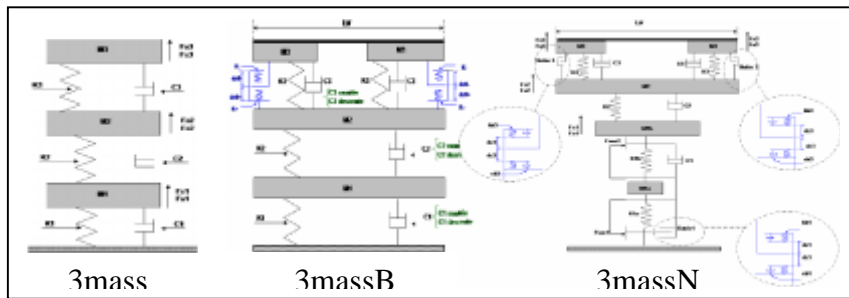


Figure 10: Pantograph lump mass models (3mass, 3massBF and 3massNL)

The simplest model is a linear 3 stages lump mass model.

The 3massBF model advantage is that the upper part has a more realistic dynamical behaviour of the bow, which allows taking into account the rotational inertia of the bow and the displacements of the bow suspensions according to the catenary stagger. This model also enables to introduce simple non-linearities, such as bumpstops or damping elements with different characteristics depending on the motion direction.

Finally, the 3massNL is the most accurate, reliable and elaborate model available in OSCAR. It uses complex equivalent rheological models. The drawback is that identifying the rheological equivalent models is a time and money consuming task.

In the following paragraphs, the influence of two kinds of such non-linearities are studied using the 3massBF model: the bumpstops and a non linear damper.

4.1 Sensitivity analysis of the upper suspension

The influence of a bumpstop clearance in the bow suspension on the displacements is depicted in Figure 8. Each graphic represents displacements in the left and right suspensions. The clearance is progressively increased: $\pm 1\text{cm}$, $\pm 2\text{cm}$, $\pm 4\text{cm}$, “no bumpstop”.

The nominal situation on the CX pantographs at SNCF is shown in the third graphic, where one can easily notice the effect of the contact wire stagger on the left and right suspension displacements. In this specific case the oscillations amplitude is lower than the bumpstop clearance, which leads to a linear behaviour equivalent to the “no bumpstop” case.

When the clearance is reduced and as soon as the limit displacement is reached, bumpstops become active and the displacement pattern is strongly modified (cf. the two first graphs).

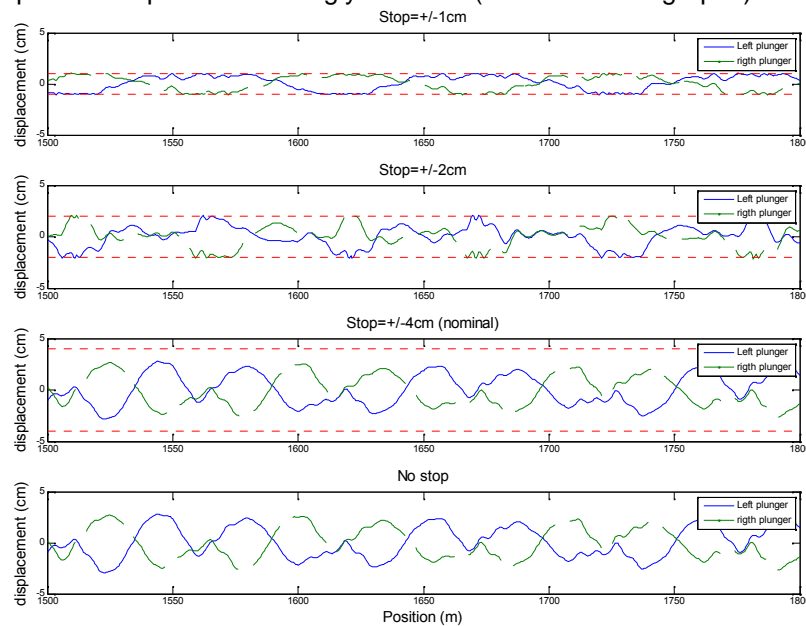


Figure 8: Influence of stops on bow suspension displacements ($\pm 1\text{cm}$, $\pm 2\text{cm}$, $\pm 4\text{cm}$, no stops).

Since the bumpstops have a strong influence on the plunger displacements, it can be thought that the bumpstops must be taken into account for a sensitivity analysis.

Challenge E: Bringing the territories closer together at higher speeds

To check this, Figure 12 presents the sensitivity of various parameters (C1,K1,M3,C3,K3) on the σ/F_m criterion in the two following cases:

- upper suspension bumpstops are taken into account,
- upper suspension bumpstops are not taken into account.

From this figure, one can notice that the upper suspension stiffness K3 is the most sensitive parameter if one does not consider the bumpstops. On the contrary, if one takes into account the design constraint linked to the presence of bumpstops (which are necessary due to the space available in this region of the pantograph), K3 becomes the less sensitive parameters.

Another conclusion of Figure 12 is that the sensitivity of parameters (C1,K1,M3,C3) can be obtained without considering the presence of bumpstops.

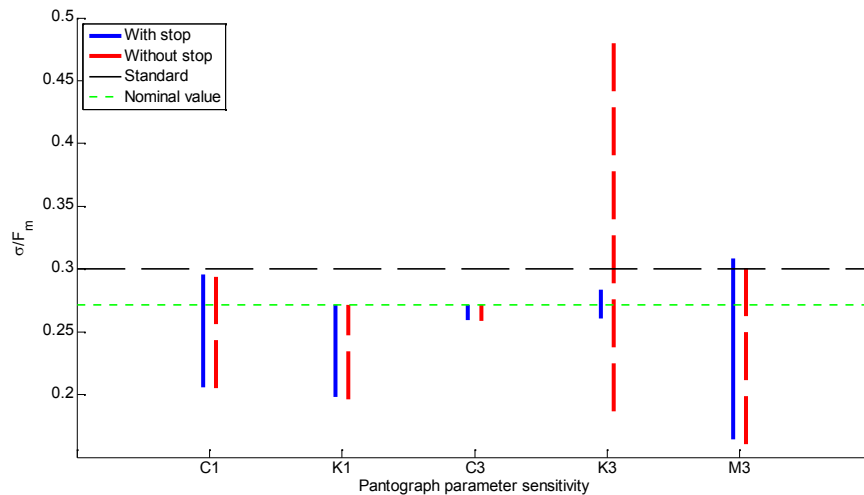


Figure 12: Bumpstop impact on pantograph sensitivity analysis.

If one intends to optimise the stiffness of the upper suspension K3, the clearance of the bumpstops must be carefully checked. Indeed, as presented in Figure 13, reducing K3 theoretically improves the performance (σ/F_m is reduced as well as the max uplift of the steady arm), but if one considers the optimum to be 100N/m, then a clearance of nearly ± 40 cm must be applied, which is totally unrealistic. On the contrary if one takes into account the bumpstop constraint, then no improvement can be obtained by modifying K3. A compromise must thus be achieved between bumpstop clearance and suspension stiffness.

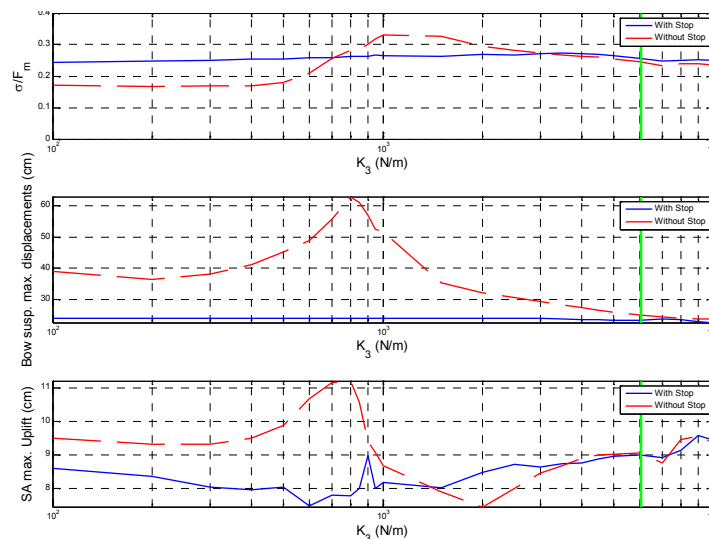


Figure 13: Influence of upper suspension bumpstops on performance criteria (vertical green line : nominal value = 6045N/m).

4.2 Sensitivity analysis of a non linear damper

Challenge E: Bringing the territories closer together at higher speeds

In actual pantographs, the lower stage damper is non linear since the damping value is usually higher downwards than upwards. Figure 14 presents a sensitivity analysis of these two damping values. It shows that the sensitivity of C1downwards is much higher than sensitivity of C1upwards.

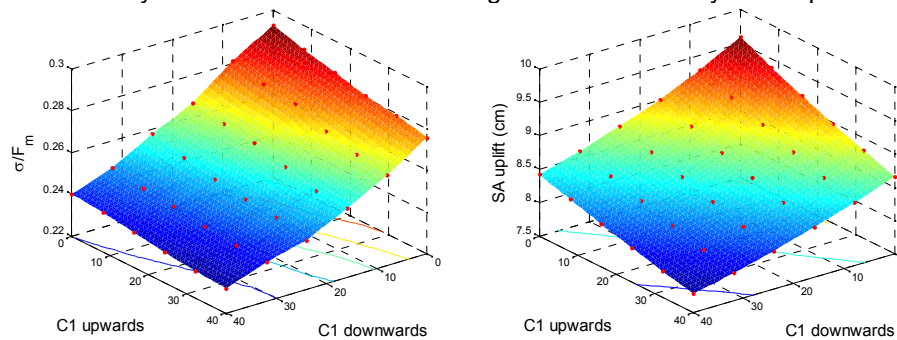


Figure 14: Non linear damping sensitivity on c/F_m and maximum steady arm uplift.

5. Catenary optimisation

5.1 Description of the application case

The aim of the optimisation is to design an optimised catenary for operating at 140km/h with two pantographs spaced of 100m.

The selected pantograph type is a Faiveley LX 1800 25kV, which parameters are described in the figure below:

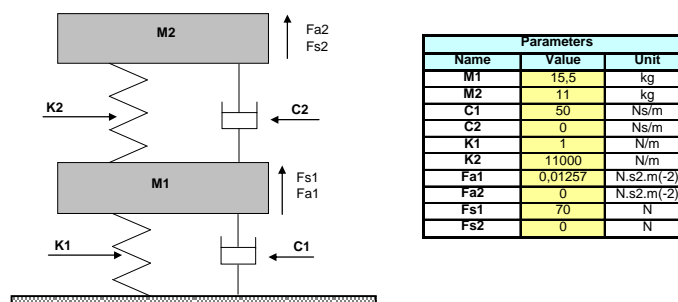


Figure 15: Pantograph parameters utilised for the parametric analysis.

The selected catenary is made of one contact wire and one messenger wire, with span lengths varying from 54 m to 58 m. Its main mechanical parameters are described below:

Parameter	Contact wire	Messenger wire
Section (m ²)	1,07E-04	6,54E-05
Linear mass (kg/m)	0,98	0,59
Young modulus (Pa)	1,20E+11	8,47E+10
Tension (N)	10000	10000

Table 2: Catenary nominal parameters.

The nominal sag coefficient of this catenary, defined as the difference in height between the span middle point and the extreme droppers, is $S=L/1000$ with L the span length of the considered span (cf. figure below).

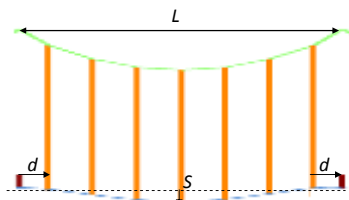


Figure 16: Definition of the sag S and of the distance of the extreme droppers from the masts (d).

5.2 Parametric analysis

In this section, a parametric analysis is performed over the following design parameters:

- Contact wire tension,

Challenge E: Bringing the territories closer together at higher speeds

- Contact wire sag coefficient (S/L, cf. Figure),
- Distance from the extreme droppers to the masts (d, cf. Figure 16).

When one parameter is varied, the others remain constant. To ensure this, the droppers length are recomputed when varying the tension or the distance d.

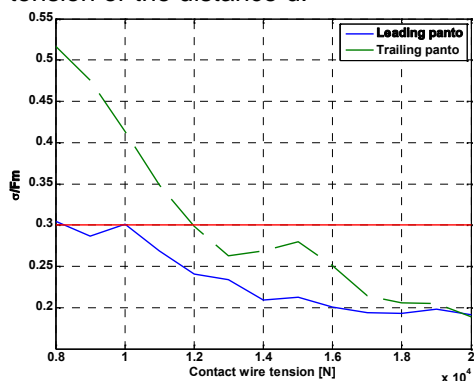


Figure 17: σ/F_m against contact wire tension ($v=140$ km/h, $1/1000$ sag)

The criteria of interest is again σ/F_m , which gives a good overview of the current collection quality. But since limitations on the steady arm maximum uplift also exist, this criterion is sometimes considered in order to indicate the boundaries which must be respected.

The evolution of σ/F_m with the contact wire tension (cf. figure below,) clearly shows the improvements that can be obtained by increasing the tension, which makes this parameter the first candidate of the design parameters.

The effect of the sag ratio S/L is also clearly visible in the top of Figure 18, which shows that an optimum is found around $S/L=10^{-3}$. The need for a certain level of sag is linked to the fact that it is intended to compensate the variation of flexibility of the catenary system, which is lower at the supports than at the middle of the spans. Moreover when determining the optimal design sag, the case when the contact wire is worn and thus lighter must be considered, which requires some extra sag.

It could be thought from the top of Figure 18 that some negative sag (around $S/L=1.5 \cdot 10^{-3}$) could lead to a local optimum, but this negative sag leads to a particularly high value of maximum uplift (cf. bottom of Figure 18), which does not allow to use such a value (a limitation on the maximum uplift is imposed at 8cm, for gauge reasons).

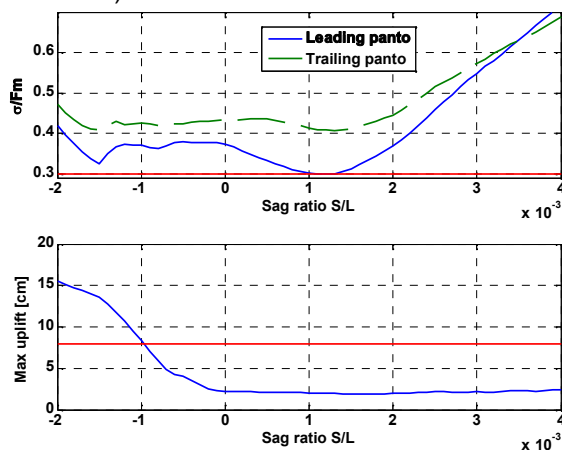


Figure 18: σ/F_m and maximum uplift against sag ratio S/L ($v=140$ km/h)

The same compromise between these two criteria must be made for what concerns parameter d (distance from the extreme droppers to the masts). Indeed, increasing this distance improves the contact force but deteriorates the maximum uplift, as can be shown in Figure 19.

Challenge E: Bringing the territories closer together at higher speeds

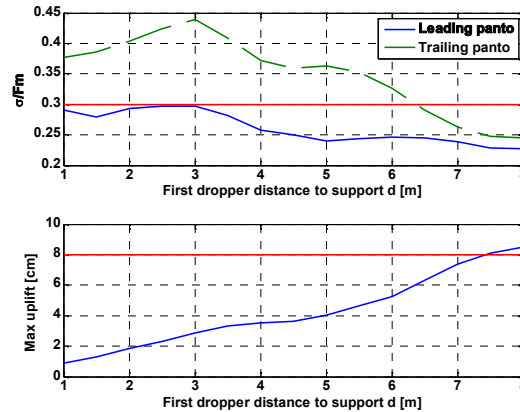


Figure 19: F/F_m and maximum uplift against first dropper distance to support d ($v=140$ km/h)

5.3 Innovative droppers

Another application of simulation consists in testing innovative solutions. Ref. [10] proposes to use dampers in the catenary in order to reduce the reflective waves and consequently improve current collection quality.

The same idea has been adapted to propose a design of droppers that would damp the catenary motion. This is of particular interest when operating with multiple pantographs, since the oscillations generated by the first pantograph impact the second pantograph.

To design the damping droppers, the first step consisted in computing the strain energy in each dropper. When pantographs are circulating under the catenary, each dropper shows a unilateral behaviour. The top of Figure presents, for one dropper, the evolution of its relative velocity (difference between the speeds of the upper and lower nodes) and of its tensile force during one simulation. The unilateral behaviour is here clearly visible. For each dropper, its strain energy is then computed by:

$$E = \int_0^T F \cdot v dt = \int_0^T [Ku + Cv]v dt,$$

with F the tensile force and v the relative velocity.

It can be checked that the droppers that have the highest strain energy are situated close to the masts (cf. bottom of Figure 20).

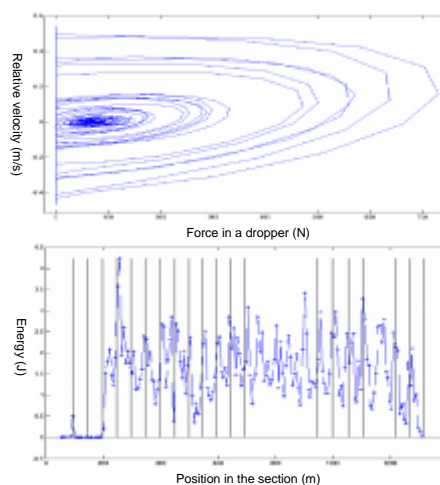


Figure 20: **Top:** Behaviour of a dropper during the passage of a pantograph. **Bottom:** Total strain energy in each dropper over the complete simulation time, depending on its position.

The idea thus consisted in placing damping droppers only close to the masts in order to dissipate energy at lower cost. A study was performed to evaluate the optimal value of damping to improve the behaviour of the second pantograph. The main result of this study is presented in Figure 21, which shows a large improvement on contact force fluctuations for the trailing pantograph.

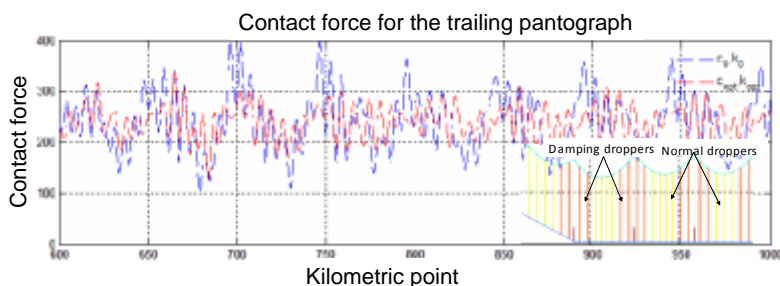


Figure 21: Effect of damping dropper on current collection – case of multiple pantographs (blue: classical droppers, red: optimal damping droppers).

6. Conclusion

The proposed article deals with the simulation of pantograph-catenary interaction. It first shows the mechanical specificities of this problematic (waves propagation, non linearities, etc.), and presents the way the OSCAR software deals with them. The second part brings a comprehensive understanding of the resonances that appear at various speeds, especially when running with multiple pantographs. Based on these theoretical parts, application cases are then proposed. In the third part, an analysis of pantograph non linearities is presented, and their impact on a sensitivity analysis is evaluated. Finally, a catenary parametric study is presented and catenary components are proposed.

7. References

- [1] A. Bobillot, L.M. Cléon, A. Collina, O. Mohamed, R. Ghidorzi, “Pantograph-Catenary: a High-Speed European couple” . In: Proceedings of the World Congress on Railway Research, 2008.
- [2] A. Bobillot, V. Delcourt, P. Demanche, J.P. Massat: “Pantograph-Catenary: three paths to knowledge”. In: Proceedings of the World Congress on Railway Research, 2006
- [3] L.M. Cléon, A. Bobillot, J.P. Mentel, E. Aziz: “OSCAR: La caténaire en 3D”. In: Revue Générale des Chemins de Fer, Volume n° 155, November 2006.
- [4] J.P. Massat, J.P. Lainé, A. Bobillot, “Pantograph-Catenary Dynamic Simulation”. Proceedings of the IAVSD conference, 2004.
- [5] J.P. Massat, A. Bobillot, J.P. Lainé, “Robust Methods for Detecting Defects in Overhead Contact Line Based on Simulation Results”, III ECCOMAS Conference 2006, Lisbon, Portugal, 5–8 June, 2006
- [6] Frederico Rauter, João Pombo, Jorge Ambrósio, Jérôme Chalansonnet, Adrien Bobillot, Manuel Seabra Pereira, “Contact Model for the Pantograph-Catenary Interaction”, International Journal of System Design and Dynamics, 2007.
- [7] J.P. Bianchi, E. Balmès, A. Bobillot, “Using modal damping for full model transient analysis. Application to pantograph/catenary vibration”, ISMA2010 Noise and Vibration Engineering conference 2010.
- [8] K. Manabe, “Periodical Dynamic Stabilities of a Catenary-Pantograph System”, QR of RTRI, vol. 35, No. 2, May 1994.
- [9] J.P. Massat, “Modélisation du comportement dynamique du couple pantographe-caténaire. Application à la détection de défauts dans la caténaire”, doctoral thesis 2007.
- [10] C. Bourgeois, “Interaction pantographe-caténaire. Analyse des phénomènes et des performances”, master report ECP/SNCF, 2010.
- [11] Z. Weihua et al., “Investigation and application on the pantograph-catenary system with double pantographs for the running speed of 350 km/h and above”, UIC High-Speed Congress, 2010.
- [12] T. Hayasaka, “Effect of reduced reflective wave propagation on overhead contact lines in overlap section”, QR of RTRI, vol. 45, No. 2, May 2004.